Engineering with Computers (2022) 38 (Suppl 4):S3251–S3268
https://doi.org/10.1007/s00366-021-01455-y

ORIGINAL ARTICLE

A particle swarm optimization and coupled generalized differential quadrature element methods with genetic algorithm for stability analysis of the laminated microsystems

Hua Sun[1]

Received: 23 April 2021 / Accepted: 13 June 2021 / Published online: 29 June 2021

Abstract
In this paper, an attempt is made to extend a linear two-dimensional model for stability analysis of the laminated annular microplate subject to external excitation. A new approach called hybrid optimization is introduced to solve optimization problems with a high sensitive objective function to decline computational costs and increase the predicted optimum results accuracy. Regarding this issue, generalized differential quadrature element method (GDQEM), particle swarm optimization (PSO), as well as genetic algorithm (GA) methods are coupled to improve the dynamic stability of the annular microsystems via finding an optimum frequency and fiber angle of layers simultaneously. Higher-order shear deformation theory (HSDT) and Hamilton's principle are taken into consideration for the exact derivation of the general linear governing equations and boundary conditions of the axisymmetric laminated annular plate. Also, modified couple stress theory (MCST) is presented for presenting the size-dependency of the current microsystem. The GDQEM is used to solve the governing equations of the microsystem via its boundary domains. To enhance the genetic algorithms' performance for solving equations, the optimizer approach of particle swarm has been employed as a GA's operator. Precise convergence and practicality of the suggested mixed-method have been disclosed. Moreover, we would have proven that for achieving the convergence PSO's and GA's outcomes, we have to apply higher than fifteen iterations.

Keywords Iteration algorithm · Particle swarm optimization · Higher-order shear deformation theory · Annular microsystem · Genetic algorithm · Frequency

1 Introduction

A broad range of engineering designers has been considerably considering laminated composites since decades ago, for instance, in mechanical and civil engineering. composites are mainly employed as the elements of heavy-load light-weight systems regarding their specific characteristics such as stiffness, high strength, and other functionalities. This kind of material can be used in various systems [1–4]. For this matter, researchers have been attending to consider laminated composites since a few decades ago. Multifarious structure types, including beams, plates, and shells, have been considered to be vibrationally analyzed by Mikhasev et al. [5]. They disclosed that shear's influence has a prominent contribution in the laminated structures' free vibrations, and for exploring future researches, they have to be taken into consideration. Ref. [6] analyzed the frequency analysis of a laminated micro-sized beam employing the modified couple stress (MCS) approach. In that reported paper, impacts of physical/geometrically factors had been considered on the mentioned system's stability. Their presented material can be used in many applications such as [7–10]. Sinha [11] reported the laminated plate's frequency investigation applying numerical and empirical techniques. They, however, revealed that their achieved outcomes from the computational approach are in a decent agreement with those empirically conducted. spinning Conical FG-CNTRC shell's vibrational behaviors have been analyzed by Ref. [12]. Then, the complicated equations have been solved employing the Kp-Ritz approach. The nonlinear vibration of a laminated plate has been scrutinized by Ref. [13]. They disclosed that for characterizing a laminated plate, number of layers and the ply directions have to be carefully considered,

✉ Hua Sun
harriet999@163.com

1 Library, Shandong University of Arts, Jinan 250014, Shandong, China

at the same time. It was illustrated that annular plates could be applied in a wide range of industrial and engineering practical applications [14]. The presented approach in the previous reference can be a good tool for the analysis of complex systems [15–19]. Employing nano-scaled reinforcements for enhancing the structures' mechanical properties have been analyzed since decades ago [20–28]. In the dynamic area of the annular plate, Civalek et al. [29] applied a first-order-shear-deformation (FOSD) approach and a semi computational technique for analyzing the sector annular plate's frequency has been investigated with assuming FG material. The mentioned solution procedure as a strong solver can be used in many systems such as [30–33]. Mohammadimehr et al. [34] reported a study on the dynamics and statics characteristics of a thin FG disk subject to primary pressure and lied in a viscoelastic condition. Their problem's formulation has been extracted by a classical approach and GDQ technique has been used as an equation solver. Arshid et al. [35] studied the FG smart disk frequency response subjected to three types of physical loads through applying semi computational technique and thick model. They made a formulation regarding electro-magneto-elastic material for their study and assumed that the smart disk would be located in a thermal area. Their outcome discloses that by raising the field of the magnet, the system would be stiffer so it would be a reason for enhancing the system's frequency. Also, this kind of analysis can be used in many systems [36–39]. Employing an FE analysis, Vinyas [40] reported research on the electro-magneto-elastic annular and circular FG plate's dynamics through applying a higher-order-shear-deformation approach and there was an analysis regarding the influences of imperfection on the mode shape and the highest deflection. Due to new demand in technology composite structures can be used as the main materials in the future [41–43]. Safarpour et al. [44] made a formulation on the characterizing the GPLs filled an FG annular plate, cylindrical and conical shell employing a 3D-elasticity method for presenting dynamic and static behavior of the system. they selected the GDQ solver approach and they claimed that the GPLs' geometric properties have a vital contribution to the structures' frequency and bending behaviors. Also, owing to the new demand in technology [45–48], the previous solution procedure is a strong tool for solving various complex structures. Dai et al. [49] analyzed a dynamics of a spinning CNTs filled annular structure by taking into account the influences of hygro-thermal condition, natural imperfection in the material, and aggregation phenomenon. They selected the GDQ approach as a solver and they presented that moisture and spinning velocity would contribute significantly to the disk's frequency. The used method of the previous reference can be a good tool for solving complex problems such as [50–54]. Eshraghi and Dag [55] employed the boundary element approach as a practical technique for analyzing the FG disk's forced vibration. Khouzestani and Khorshidvand [56] scrutinized the frequency and bending of the axisymmetric imperfected disk by using the basic shear deformation method and variational approach. Their outcomes disclosed that as the imperfection raises, the stress field and frequency would be reduced. Javani et al. [57] studied thermal buckling investigation of a sector GPLs filled FG disk by applying a first-order model and a semi computational approach. Moreover, they used configurational nonlinearity employing von Kármán theory. As they revealed, GPLs would boost the critical temperature and buckling load of the imperfect disk. Heshmati et al. [58] extracted the equations of a sandwich disk considering imperfections as porosities in its material and analyzed the natural frequencies by applying the FOSD model and Chebyshev theory. They finally asserted that porosity's density in the sandwich disk's core would indirectly affect the structure's frequency. Since nano science has been developed in multifarious industries. Specifically, in the area of NEMS and MEMS, size effect consideration to estimate the thermomechanical characteristics of the nano-scaled structures has become a vital issue [59–69]. Due to the aforementioned fact, Bidgoli et al. [70] by applying nonlocal modified strain gradient analyzed the vibration characteristics of a micro-scaled plate which is supposed that the material of the system is FG. They, however, revealed that their formulated relation has been solved through applying an analytical approach. The presented approach in the previous reference can be a good tool for the analysis of complex systems [71–74]. Mahinzare et al. [75] presented a complete study on the electrically FG disk's dynamics in a thermal condition through using the FOSD model and nonlocal-strain-gradient approach. Moreover, they revealed the influences of the nonlocal-strain-gradient model and Eringen on the smart structure's frequency. they selected the GDQ approach as a solver for illustrating their outcomes. This kind of analysis can be used in many structures and systems such as [76–80]. Arshid et al. [81] applied modified-strain-gradient, and FOSD models for analyzing stability and frequency behavior of a GPLs filled annular micro-scaled system. Their extended equations were finally solved through using the GDQ technique and they demonstrated that the viscoelastic substrate and thermal condition would be able to considerably affect the mechanics of the small-sized disk. Pal and Das [82] formulated the boundary conditions and motion equations of a spinning annular FG micro-scaled system by employing modified couple stress, Kirchhoff models, and variational methods. They assumed that the system lies in a thermal condition and they reported the disk's shape mode in multifarious conditions. EmployingKirchhoff and nonlocal-strain-gradient models, Huang et al. [83] scrutinized the dynamic characteristics of an annular electrical micro-scaled system. They presented the influences of strain gradient on the vibration and bending behavior by extracting the equations with the lowest potential energy technique. Alinaghizadeh and Shariati [84] investigated nonlinear micro-sized sector plate's mechanics by applying MCST. They combined that the system with a viscoelastic substrate and the strain–stress equations have been extracted by employing the classical approach. They disclosed that size dependency and nonlinearity would have the most considerable influences on the annular plate's bending. The presented approach in the previous reference can be a good tool for the analysis of medical problems [85–90]. Mohammadimehr et al. [91] presented a complete analysis on the electro-mechanical annular sandwich micro-sized structure's buckling in which CNTs have been employed as fillers. They assumed the size dependency applying the modified-strain-gradient model and achieved the BCs and governing equations through employing lowest energy approach. They revealed that the nonlocal and electric potential impacts would contribute significantly to the smart disk's stability prediction. Alipour et al. [92] analyzed one of their study for studying the nano/micro annular sandwich system's statics applying a new nonlocal technique called the zigzag approach. the annular isotropic rotary micro-sized system's motion equation through multifarious continuum models has been presented by Bagheri et al. [93]. They disclosed that the crucial angular velocity raises with each raise in the nonlocal factor. Recently, using various methods for solving the dynamics of various structures has got a lot of attention among the researchers [94, 95]. Regarding this issue, stability analysis of various structures is investigated by many researchers [96–103]. According to the aforementioned literature review, definitely there is no published paper amongst researchers' publications for analyzing the dynamic stability of the annular micro systems via finding optimum frequency, and fiber angle of layers via GDQE, PSO, and GA methods. Thus, in the presented scrutinization, frequency characteristics of an annular micro-scaled plate are analyzed by detail. For this matter, PSO, FSE, and GA approaches are combined for studying the frequency of an annular microplate via finding optimum frequency value. The HOSD model has been employed to make the formulation of the stress–strain equations. By applying the variational approach, the structure's governing equations are extracted. Then, to analyze the impacts of configurational elements of the laminated system and mechanics influence on the annular plate's frequency, aparametric study is conducted.

2 Mathematical modeling

A laminated annular system is shown in Fig. 1. The inner, and outer radius of the microsystem is shown with R_i and R_o, respectively. Also, $\bar{\theta}$ is fiber angle of the laminated material.

In the current research, the displacement fields can be given as follows [104]

$$\alpha^{\eta} = \alpha_0^{\eta} + z\chi_R^{\eta} - C_1 z^3\left(\chi_R^{\eta} + \partial_R\left(\gamma_0^{\eta}\right)\right) \tag{1}$$

$$\beta^{\eta} = \beta_0^{\eta} + z\chi_{\theta}^{\eta} - C_1 z^3\left(\chi_{\theta}^{\eta} + R^{-1}\partial_{\theta}\left(\gamma_0^{\eta}\right)\right)$$

$$\gamma^{\eta} = \gamma_0^{\eta}$$

According to the HSDT, C_1 is $4/3h^2$. The stress–strain relations for the laminated system are as below:

$$\begin{Bmatrix} \sigma_{RR} \\ \sigma_{\theta\theta} \\ \tau_{R\theta} \\ \tau_{Rz} \\ \tau_{\theta z} \end{Bmatrix} = \begin{bmatrix} \hat{\bar{Q}}_{11} & \hat{\bar{Q}}_{12} & 0 & 0 & \hat{\bar{Q}}_{16} \\ \hat{\bar{Q}}_{21} & \hat{\bar{Q}}_{22} & 0 & 0 & \hat{\bar{Q}}_{26} \\ 0 & 0 & \hat{\bar{Q}}_{44} & \hat{\bar{Q}}_{45} & 0 \\ 0 & 0 & \hat{\bar{Q}}_{45} & \hat{\bar{Q}}_{55} & 0 \\ \hat{\bar{Q}}_{16} & \hat{\bar{Q}}_{26} & 0 & 0 & \hat{\bar{Q}}_{66} \end{bmatrix} \begin{Bmatrix} \varepsilon_{RR} \\ \varepsilon_{\theta\theta} \\ \gamma_{R\theta} \\ \gamma_{Rz} \\ \gamma_{\theta z} \end{Bmatrix} \tag{2}$$

here the factors of the $_{ij}$ matrix, pertained to the orthotropic material associated to Lth lamina, would be explained as:

$$\hat{\bar{Q}}_{11} = \cos^4\bar{\theta}\tilde{Q}_{11} + 2\sin^2\bar{\theta}\cos^2\bar{\theta}\left(\tilde{Q}_{12} + 2\tilde{Q}_{66}\right) + \sin^4\bar{\theta}\tilde{Q}_{22} \tag{3a}$$

$$\hat{\bar{Q}}_{12} = \sin^2\bar{\theta}\cos^2\bar{\theta}\left(\tilde{Q}_{11} + \tilde{Q}_{22} - 4\tilde{Q}_{66}\right) + \left(\sin^4\bar{\theta} + \cos^4\bar{\theta}\right)\tilde{Q}_{12} \tag{3b}$$

$$\hat{\bar{Q}}_{16} = \cos^3\bar{\theta}\sin\bar{\theta}\left(2\tilde{Q}_{11} - 2\tilde{Q}_{12} - \tilde{Q}_{66}\right) + \cos\bar{\theta}\sin^3\bar{\theta}\left(\tilde{Q}_{66} + 2\tilde{Q}_{12} - 2\tilde{Q}_{22}\right) \tag{3c}$$

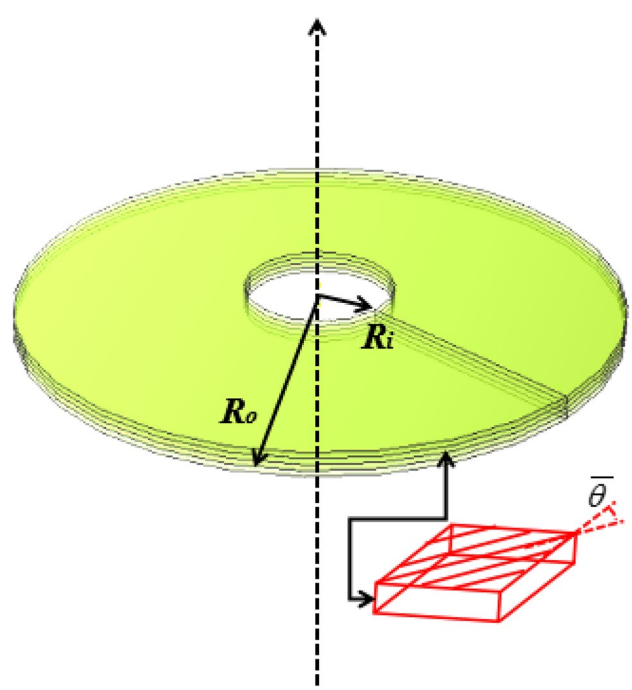

Fig. 1 A schematic view of laminated annular microsystem

$$\hat{\bar{Q}}_{22} = \sin^4\bar{\theta}\tilde{Q}_{11} + 2\sin^2\bar{\theta}\cos^2\bar{\theta}\tilde{Q}_{12} + \cos^4\bar{\theta}\tilde{Q}_{22} + 2\sin^2\bar{\theta}\cos^2\bar{\theta}\left(\tilde{Q}_{12} + 2\tilde{Q}_{66}\right) \quad (3d)$$

$$\hat{\bar{Q}}_{26} = \cos^3\bar{\theta}\sin\bar{\theta}\left(2\tilde{Q}_{12} - 2\tilde{Q}_{22} + \tilde{Q}_{66}\right) + \cos\bar{\theta}\sin^3\bar{\theta}\left(2\tilde{Q}_{11} - 2\tilde{Q}_{12} - \tilde{Q}_{66}\right) \quad (3e)$$

$$\hat{\bar{Q}}_{44} = \cos^2\bar{\theta}\tilde{Q}_{44} + \sin^2\bar{\theta}\tilde{Q}_{55} \quad (3f)$$

$$\hat{\bar{Q}}_{45} = \cos\bar{\theta}\sin\bar{\theta}\left(\tilde{Q}_{55} - \tilde{Q}_{44}\right) \quad (3g)$$

$$\hat{\bar{Q}}_{55} = \cos^2\bar{\theta}\tilde{Q}_{55} + \sin^2\bar{\theta}\tilde{Q}_{44} \quad (3h)$$

$$\hat{\bar{Q}}_{66} = \tilde{Q}_{66}\left(\cos^2\bar{\theta} - \sin^2\bar{\theta}\right)^2 + 4\sin^2\bar{\theta}\cos^2\bar{\theta}\left(\tilde{Q}_{11} + \tilde{Q}_{22} - 2\tilde{Q}_{12}\right) \quad (3i)$$

As it is already mentioned, the equations written by Eq. (3) would be stress–strain constitutive equations for the Lth orthotropic lamina, which could be referred to as material in $x,y,$ and z directions. In Eq. (3), θ would be fiber orientation angle and Q_{ij} would be written as [105, 106]:

$$\tilde{Q}_{11} = \frac{E_1}{1-\nu_{12}\nu_{21}},\quad \tilde{Q}_{12} = \frac{\nu_{12}E_2}{1-\nu_{12}\nu_{21}},\quad \tilde{Q}_{22} = \frac{E_2}{1-\nu_{12}\nu_{21}}$$
$$\tilde{Q}_{66} = G_{12},\quad \tilde{Q}_{44} = G_{23},\quad \tilde{Q}_{55} = G_{13} \quad (4)$$

So, the strain components of the laminated layers can be given by:

$$\varepsilon^c_{RR} = \partial_R\alpha^c_0 + z\partial_R\chi^c_R - C_1z^3\left(\partial_R\chi^c_R + \partial^2_R\gamma^c_0\right) \quad (5a)$$

$$\varepsilon^c_{\theta\theta} = R^{-1}\alpha^c_0 + R^{-1}\partial_\theta\beta^c_0 + zR^{-1}\left(\chi^c_R + \partial_\theta\chi^c_\theta\right) - C_1z^3R^{-1}\left(\left(\chi^c_R + \partial_R\gamma^c_0\right) + \left(\partial_\theta\chi^c_\theta + R^{-1}\partial^2_\theta\gamma^c_0\right)\right) \quad (5b)$$

$$\begin{aligned}\gamma^c_{R\theta} =& R^{-1}\partial_\theta\alpha^c_0 + \partial_R\beta^c_0 - R^{-1}\beta^c_0 \\ &+ z\left(R^{-1}\partial_\theta\chi^c_R + \partial_R\chi^c_\theta - R^{-1}\chi^c_\theta\right) \\ &- z^3C_1\left(R^{-1}\left(\partial_\theta\chi^c_R + \partial^2_{R\theta}\gamma^c_0\right)\right. \\ &+\left(\partial_R\chi^c_\theta + R^{-1}\partial^2_{R\theta}\gamma^c_0\right) \\ &\left.-R^{-1}\left(\chi^c_\theta + R^{-1}\partial_\theta\gamma^c_0\right)\right)\end{aligned} \quad (5c)$$

$$\gamma^c_{Rz} = \chi^c_R + \partial_R\gamma^c_0 - 3C_1z^2\left(\chi^c_R + \partial_R\gamma^c_0\right) \quad (5d)$$

$$\gamma^c_{\theta z} = \chi^c_\theta + R^{-1}\partial_\theta\gamma^c_0 - 3C_1z^2\left(\chi^c_\theta + R^{-1}\partial_\theta\gamma^c_0\right) \quad (5e)$$

2.1 Hamilton's principle

For obtaining the nonlinear governing equations and general boundary equations of the system, we used Hamilton's principle as follows [107, 108]:

$$\int_{t_1}^{t_2}\left(\delta T - \delta U + \delta V_1 + \delta V_2 + \delta V_3\right)^\eta dt = 0 \quad (6)$$

The strain formulations of the current system can be given as below [109–112]:

$$\delta U^c = \int_V \sigma^c_{ij}\delta\varepsilon^c_{ij}dV =$$
$$\int_{R_1}^{R_2}\int_0^\theta\left(\begin{aligned}&\left\{\partial_RN_{RR} + R^{-1}\partial_\theta N_{R\theta} - R^{-1}N_{\theta\theta}\right\}\delta\alpha_0 + \left\{R^{-1}\partial_\theta N_{\theta\theta} + \partial_\theta N_{R\theta} + R^{-1}N_{R\theta}\right\}\delta\beta_0 \\ &\left\{\begin{aligned}&C_1\partial^2_RP_{RR} - R^{-1}C_1\partial_RP_{\theta\theta} + R^{-2}C_1\partial^2_\theta P_{\theta\theta} + 2C_1R^{-1}\partial^2_{R\theta}P_{R\theta} \\ &+C_1R^{-2}\partial_\theta P_{R\theta} + \partial_RS_{RZ} - 3C_1\partial_RQ_{RZ} + R^{-1}\partial_\theta S_{\theta Z} - 3C_1R^{-1}\partial_\theta Q_{\theta Z}\end{aligned}\right\}\delta\gamma_0 \\ &+\left\{\begin{aligned}&\partial_RM_{RR} - C_1\partial_RP_{RR} - R^{-1}M_{\theta\theta} + C_1R^{-1}P_{\theta\theta} \\ &+R^{-1}\partial_\theta M_{R\theta} - C_1R^{-1}\partial_\theta P_{R\theta} - \left(S_{RZ} + 3c_1Q_{RZ}\right)\end{aligned}\right\}\delta\chi_R \\ &+\left\{\begin{aligned}&R^{-1}\partial_\theta M_{\theta\theta} - R^{-1}C_1\partial_\theta P_{\theta\theta} + \partial_RM_{R\theta} - C_1\partial_RP_{R\theta} \\ &+R^{-1}M_{R\theta} - R^{-1}C_1P_{R\theta} + R^{-1}M_{R\theta} - R^{-1}C_1\partial_\theta P_{R\theta} - S_{\theta Z} + 3c_1Q_{\theta Z}\end{aligned}\right\}\delta\chi_\theta\end{aligned}\right)RdRd\theta \quad (7)$$

where:

$$\{N_{RR}, M_{RR}, P_{RR}\} = \int_z \sigma_{RR}\{1, z, z^3\}dz \tag{8a}$$

$$\{N_{\theta\theta}, M_{\theta\theta}, P_{\theta\theta}\} = \int_z \sigma_{\theta\theta}\{1, z, z^3\}dz \tag{8b}$$

$$\{N_{R\theta}, M_{R\theta}, P_{R\theta}\} = \int_z \sigma_{R\theta}\{1, z, z^3\}dz \tag{8c}$$

$$\{Q_{RZ}, S_{RZ}\} = \int_z \sigma_{RZ}\{z^2, 1\}dz \tag{8d}$$

$$\{Q_{\theta Z}, S_{\theta Z}\} = \int_z \sigma_{\theta Z}\{z^2, 1\}dz \tag{8e}$$

The variation of the work done can be given as below:

$$\delta V_2^\eta = \int_A q_{dynamic}\delta w^\eta dA \tag{9}$$

where q can be given as below:

$$q_{dynamic} = F \times \cos(\Omega t) \tag{10}$$

The kinetic energy's first variation would be given as:

$$T = \frac{1}{2}\int_V \rho\left[(\partial_t\alpha)^2 + (\partial_t\beta)^2 + (\partial_t\gamma)^2\right]dV \tag{11}$$

where $\{I_i\} = \int_{-\frac{h}{2}}^{\frac{h}{2}} \{z^k\} \times \rho^{NCM} \times dz,\ \ k = 1 : 6$. Now by replacing Eqs. (12), (10), (9), and (7) into Eq. (6) the motion equations of the current system can be given as follows:

$$\begin{aligned}\delta\alpha_0 :\ & \partial_R N_{RR} + R^{-1}\partial_\theta N_{R\theta} - R^{-1}N_{\theta\theta} \\ &= I_0\partial_t^2\alpha_0 + I_1\partial_t^2\chi_R - I_3c_1\left(\partial_t^2\phi_R + \partial_{Rtt}^3\gamma_0\right)\end{aligned} \tag{13a}$$

$$\begin{aligned}\delta\beta_0 :\ & R^{-1}\partial_\theta N_{\theta\theta} + \partial_\theta N_{R\theta} + R^{-1}N_{R\theta} \\ &= I_1\partial_t^2\beta_0 + I_2\partial_t^2\chi_\theta - I_3c_1\left(\partial_t^2\phi_\theta + R^{-1}\partial_{\theta t}^2\gamma_0\right)\end{aligned} \tag{13b}$$

$$\begin{aligned}\delta\gamma_0 :\ & C_1\partial_R^2P_{RR} - C_1R^{-1}\partial_RP_{\theta\theta} + C_1R^{-2}\partial_\theta^2P_{\theta\theta}^\eta \\ &+2C_1R^{-1}\partial_{R\theta}^2P_{R\theta} + C_1R^{-2}\partial_\theta P_{R\theta} \\ &+\partial_RS_{RZ} - 3C_1\partial_RQ_{RZ} + R^{-1}\partial_\theta S_{\theta Z} - 3C_1R^{-1}\partial_\theta Q_{\theta Z} - q \\ &= c_1I_3\partial_{Rtt}^3\alpha_0 + c_1I_4\partial_{Rtt}^3\chi_R - I_6C_1^2\left(\partial_{Rtt}^3\chi_R + \partial_{RRtt}^4\gamma_0\right) \\ &+C_1I_3R^{-1}\partial_{\theta tt}^3\beta_0 + C_1I_4R^{-1}\partial_{\theta tt}^3\chi_\theta \\ &-I_6C_1^2R^{-1}\left(\partial_{\theta tt}^3\chi_\theta + R^{-1}\partial_{\theta\theta tt}^4\gamma_0\right) + I_0\partial_t^2\gamma_0\end{aligned} \tag{13c}$$

$$\begin{aligned}\delta\chi_R :\ & \partial_RM_{RR} - C_1\partial_RP_{RR} - R^{-1}M_{\theta\theta} \\ &+ C_1R^{-1}P_{\theta\theta} + R^{-1}\partial_\theta M_{R\theta} \\ &- R^{-1}C_1\partial_\theta P_{R\theta} - \left(S_{RZ} + 3c_1Q_{RZ}\right) \\ &= -c_1I_3\partial_t^2\alpha_0 - c_1I_4\partial_t^2\chi_R \\ &+ I_6c_1^2\left(\partial_t^2\chi_R + \partial_{Rtt}^3\gamma_0\right) + I_1\partial_t^2\alpha_0 \\ &+ I_2\partial_t^2\chi_R - I_4c_1\left(\partial_t^2\chi_R + \partial_{Rtt}^2\gamma_0\right)\end{aligned} \tag{13d}$$

$$\delta T = \int_{R_1}^{R_2}\int_0^\theta \left[\begin{aligned} &\left\{-I_0\partial_t^2\alpha_0 - I_1\partial_t^2\chi_R + I_3c_1\left(\partial_t^2\chi_R + \partial_{Rtt}^3\gamma_0\right)\right\}\delta\alpha_0 \\ &+\left\{-I_1\partial_t^2\beta_0 - I_2\partial_t^2\chi_\theta + I_3c_1\left(\partial_t^2\chi_\theta + R^{-1}\partial_{\theta tt}^3\gamma_0\right)\right\}\delta\beta_0 \\ &+\left\{-c_1I_3\partial_{Rtt}^3\alpha_0 - c_1I_4\partial_{Rtt}^3\chi_R + I_6c_1^2\left(\partial_{Rtt}^3\chi_R + \partial_{RRtt}^4\gamma_0\right)\right\}\delta\gamma_0 \\ &+\left\{\begin{aligned} &-C_1I_3R^{-1}\partial_{\theta tt}^3\beta_0 - C_1I_4R^{-1}\partial_{\theta tt}^3\chi_\theta \\ &+I_6c_1^2R^{-1}\left(\partial_{\theta tt}^3\chi_\theta + R^{-1}\partial_{\theta\theta tt}^4\gamma_0\right)\end{aligned}\right\}\delta\gamma_0 + \left\{-I_0\partial_t^2\gamma_0\right\}\delta\gamma_0 \\ &+\left\{c_1I_3\partial_t^2\alpha_0 + c_1I_4\partial_t^2\chi_R - I_6c_1^2\left(\partial_t^2\chi_R + \partial_{Rtt}^3\gamma_0\right)\right\}\delta\chi_R \\ &+\left\{-I_1\partial_t^2\alpha_0 - I_2\partial_t^2\chi_R + I_4c_1\left(\partial_t^2\chi_R + \partial_{Rtt}^3\gamma_0\right)\right\}\delta\chi_R \\ &+\left\{-I_1\partial_t^2\beta_0 - I_2\partial_t^2\chi_\theta + I_4c_1\left(\partial_t^2\chi_\theta + R^{-1}\partial_{\theta tt}^3\gamma_0\right)\right\}\delta\chi_\theta \\ &+\left\{c_1I_3\partial_t^2\beta_0 + c_1I_4\partial_t^2\chi_\theta - I_6c_1^2\left(\partial_t^2\chi_\theta + R^{-1}\partial_{\theta tt}^3\gamma_0\right)\right\}\delta\chi_\theta \end{aligned}\right]^C RdRd\theta \tag{12}$$

$$\begin{aligned}\delta\chi_\theta\ :\ & R^{-1}\partial_\theta M_{\theta\theta} - C_1R^{-1}\partial_\theta P_{\theta\theta} + \partial_R M_{R\theta}\\ & - C_1\partial_R P_{R\theta} + R^{-1}M_{R\theta} - C_1R^{-1}P_{R\theta}\\ & + R^{-1}M_{R\theta} - C_1R^{-1}\partial_\theta P_{R\theta} - S_{\theta Z} + 3c_1Q_{\theta Z}\\ & = I_1\partial_t^2\beta_0 + I_2\partial_t^2\chi_\theta\\ & - I_4c_1\left(\partial_t^2\chi_\theta + R^{-1}\partial_{\theta tt}^2\gamma_0\right) - c_1I_3\partial_t^2\beta_0\\ & - c_1I_4\partial_t^2\chi_\theta + I_6c_1^2\left(\partial_t^2\chi_\theta + R^{-1}\partial_{\theta tt}^2\gamma_0\right)\end{aligned} \tag{13e}$$

For general boundary conditions have:

$$\delta\alpha_0 = 0 \text{ or } \mathrm{N}_{RR}\hat{n}_R + R^{-1}\mathrm{N}_{R\theta}\hat{n}_\theta = 0 \tag{14a}$$

$$\delta\beta_0 = 0 \text{ or } \mathrm{N}_{R\theta}\hat{n}_R + R^{-1}\mathrm{N}_{\theta\theta}\hat{n}_\theta = 0 \tag{14b}$$

$$\delta\gamma_0 = 0 \text{ or } \begin{bmatrix} C_1\partial_R P_{RR} + \mathrm{N}_{RR}\partial_R w - C_1R^{-1}P_{\theta\theta} + C_1R^{-1}\partial_\theta P_{R\theta}\\ +\left(S_{RZ} - 3C_1Q_{RZ}\right)\end{bmatrix}\hat{n}_R + \begin{bmatrix} C_1R^{-2}\partial_\theta P_{\theta\theta} + C_1R^{-1}\partial_R P_{R\theta} + C_1R^{-2}P_{R\theta}\\ +R^{-1}\left(S_{\theta Z} - 3C_1Q_{\theta Z}\right)\end{bmatrix}\hat{n}_\theta = 0 \tag{14c}$$

$$\delta\chi_R = 0 \text{ or } \left[\mathrm{M}_{RR} - C_1\mathrm{P}_{RR}\right]\hat{n}_R + \left[R^{-1}\mathrm{M}_{R\theta} - R^{-1}C_1\mathrm{P}_{R\theta}\right]\hat{n}_\theta = 0 \tag{14d}$$

2.2 Modified couple stress theory

For considering the size-dependency, MCST with one length scale parameter is presented. As studied in Ref. [113] for considering the MCST, the strain energy can be expressed as follows:

$$\delta U_2 = \iiint_V (m_{ij}^s\delta\chi_{ij}^s)r\,dr d\theta dz \tag{15}$$

The parameters that are introduced in Eq. (15) presented in Ref. [113]. Besides, χ_{ij}^s and m_{ij} parameters can be given by:

$$\begin{aligned}\chi_{ij}^s &= \frac{1}{2}(\varphi_{i,j} + \varphi_{j,i})\\ m_{ij}^s &= 2l^2\mu\chi_{ij}^s\end{aligned} \tag{16}$$

In Eq. (16), l represents the length scale parameter of the current microstructure. Finally, by combining the Eq. (15) into motion equations of the classical plate, the motion equations and boundary conditions of the annular microplate can be obtained.

2.3 Procedure to obtain the solution

GDQEM would be one of the most reliable computational approaches which is known for its convergence and accuracy. GDQE approach can be used for solving many systems such as [114–117]. The first assumption in this is as follows [118]:

$$\left.\frac{\partial f}{\partial r}\right|_{r=r_i,\,\theta=\theta_j} = \sum_{m=1}^{N_r}\sum_{n=1}^{N_\theta} A_{im}^r I_{jn}^\theta f_{mn} \tag{17a}$$

$$\left.\frac{\partial f}{\partial \theta}\right|_{r=r_i,\,\theta=\theta_j} = \sum_{m=1}^{N_r}\sum_{n=1}^{N_\theta} I_{im}^r A_{jn}^\theta f_{mn} \tag{17b}$$

$$\frac{\partial}{\partial r}\left(\left.\frac{\partial f}{\partial \theta}\right|_{r=r_i,\,\theta=\theta_j}\right) = \sum_{m=1}^{N_r}\sum_{n=1}^{N_\theta} A_{im}^r A_{jn}^\theta f_{mn} \tag{17c}$$

$$\left.\frac{\partial^2 f}{\partial r^2}\right|_{r=r_i,\,\theta=\theta_j} = \sum_{m=1}^{N_r}\sum_{n=1}^{N_\theta} B_{im}^r I_{jn}^\theta f_{mn} \tag{17d}$$

$$\left.\frac{\partial^2 f}{\partial \theta^2}\right|_{r=r_i,\,\theta=\theta_j} = \sum_{m=1}^{N_r}\sum_{n=1}^{N_\theta} I_{im}^r B_{jn}^\theta f_{mn} \tag{17e}$$

Also, I_{im}^r and I_{jn}^θ are equal to one when i = m and j = n, otherwise, are equal to zero. Also, A_{im}^r, A_{jn}^θ, B_{im}^r and B_{jn}^θ are first and second-order derivatives weighting coefficients through r and θ orientations, respectively, and can be given as.

$$A_{im}^r = \begin{cases} \dfrac{\xi(r_i)}{(r_i - r_m)\xi(r_m)} & when \quad i \neq m\\ -\displaystyle\sum_{k=1,k\neq i}^{N_r} A_{ik} & when \quad i = m\end{cases} \qquad i,m = 1,2,\ldots,N_r \tag{18a}$$

$$A_{jn}^\theta = \begin{cases} \dfrac{\xi(\theta_j)}{(\theta_j - \theta_n)\xi(\theta_n)} & when \quad j \neq n\\ -\displaystyle\sum_{k=1,k\neq j}^{N_\theta} A_{jk} & when \quad j = n\end{cases} \qquad j,n = 1,2,\ldots,N_\theta \tag{18b}$$

in which.

$$\xi(r_i) = \prod_{k=1,k\neq i}^{N_r}(r_i - r_k) \tag{19a}$$

$$\xi(\theta_j) = \prod_{k=1,k\neq j}^{N_\theta}(\theta_j - \theta_k) \tag{19b}$$

And.

$$B_{im}^r = 2\left(A_{ii}^r A_{im}^r - \frac{A_{im}^r}{(r_i - r_m)}\right) \quad i,m = 1,2,\ldots,N_r\ ,\ i \neq m \tag{20a}$$

$$B_{jn}^\theta = 2\left(A_{jj}^\theta A_{jn}^\theta - \frac{A_{jn}^\theta}{(\theta_j - \theta_n)}\right) \quad j,n = 1,2,\ldots,N_\theta\ ,\ j \neq n \tag{20b}$$

$$B^r_{ii} = -\sum_{k=1,k\neq i}^{N_r} B^r_{ik} \quad, i = 1,2,\ldots,N_r,\ \ i = m \tag{20c}$$

$$B^\theta_{jj} = -\sum_{k=1,k\neq j}^{N_\theta} B^\theta_{jk} \quad, j = 1,2,\ldots,N_j,\ \ j = n \tag{20d}$$

In the present study, a non-uniform set of seeds is selected through r and θ orientations as follows [119]:

$$r_i = \frac{R_0 - R_i}{2\times(el)_R}\left(1-\cos\left(\frac{(i-1)}{(N_r-1)}\pi\right)\right) + R_i \quad i = 1,2,3,\ \ldots\ ,N_r \tag{21a}$$

$$\theta_j = \frac{\chi}{2\times(el)_\theta}\left(1-\cos\left(\frac{(j-1)}{(N_\theta-1)}\pi\right)\right) \quad j = 1,2,3,\ldots,N_\theta \tag{21b}$$

In which $(el)_R$, and $(el)_\theta$ refer to the number of elements along with radius and angle directions, respectively. To solve the nonlinear governing equations, we divided the time-displacement fields of these equations to time, and displacement fields, separately, so:

$$\alpha^\eta_0(R,\theta,t) = \alpha^\eta_0(R,\theta)e^{i\omega t} \tag{22a}$$

$$\beta^\eta_0(R,\theta,t) = \beta^\eta_0(R,\theta)e^{i\omega t} \tag{22b}$$

$$\gamma^\eta_0(R,\theta,t) = \gamma^\eta_0(R,\theta)e^{i\omega t} \tag{22c}$$

$$\chi^\eta_R(R,\theta,t) = \chi^\eta_R(R,\theta)e^{i\omega t} \tag{22d}$$

$$\chi^\eta_\theta(R,\theta,t) = \chi^\eta_\theta(R,\theta)e^{i\omega t} \tag{22e}$$

After applying the GDQEM, have:

$$\left\{\left[\begin{bmatrix}M_{dd}\\M_{bd}\end{bmatrix}\ \begin{bmatrix}M_{db}\\M_{bb}\end{bmatrix}\right]\omega_n^2 + \left[\begin{bmatrix}K_{dd}\\K_{bd}\end{bmatrix}\ \begin{bmatrix}K_{db}\\K_{bb}\end{bmatrix}\right]\right\}\begin{Bmatrix}\delta_d\\\delta_b\end{Bmatrix} = 0 \tag{23}$$

here, b and d are, respectively, the boundary and domain nodes. Ultimately, displacement fields, and frequency characteristics of the system would be achieved by using GDQEM and solving the following equation,

$$K^* + M^*\omega_n^2 = 0 \tag{24}$$

where

$$K^* = [K_{bd}] - [K_{bb}][K_{db}]^{-1}[K_{dd}] \tag{25a}$$

$$M^* = [M_{bd}] - [M_{bb}][K_{db}]^{-1}[K_{dd}] \tag{25b}$$

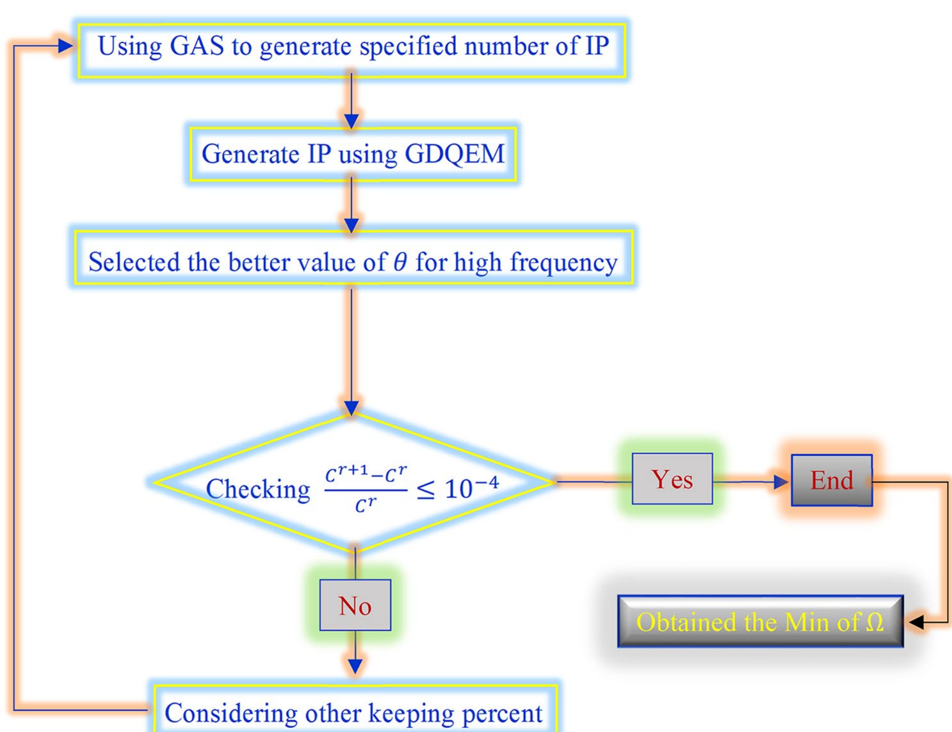

Fig. 2 Flowchart of iteration process

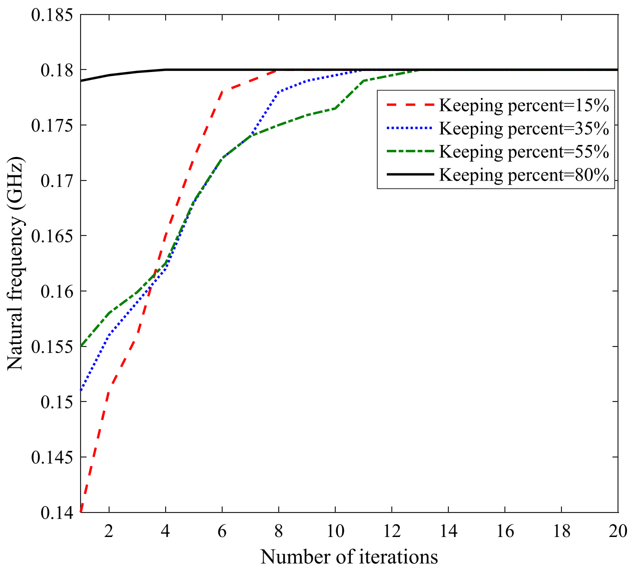

Fig. 3 Convergency of the current hybrid technique for phase speed of a sandwich plate for multifarious keeping percent

3 Results and discussion

To reveal the global annular laminated plate's highest frequency, particle swarm optimization (PSO)[120] and combined genetic algorithms (GAs) approaches [121] are applied. This combined approach is modified to overcome the disadvantages of the classical optimization approach and to enhance the genetic algorithms optimizer [121]. Some researchers used computer modeling for the analysis of various systems [122–127]. The introduced hybrid technique's solution process to maximize the crucial angular speed of the system is reported as Fig. 2.

More information in the PSO and GAs approaches may be found in Ref. [121].

In Fig. 3, the convergence of the combined introduced optimizer with multifarious keeping, percent has been shown. Using an optimization algorithm can solve complex equations [128–131]. The population number is assumed 65 in this diagram and the optimizers. According to the mentioned figure it would be quite proven that just after a few iterations numbers, the method has been converged and optimum outcomes have been achieved. Then, it is clear that by raising the population keeping percent more swift solution convergency would be likely to be obtained. In other words, the PSO approach has revised the GAs solution process. Moreover, the current optimization's flowchart would be reported as Fig. 4. From Fig. 4 can be found that a computer simulation is a strong tool for modeling a structure [132–136]. As well as this, genetic algorithm is a strong tool for simulating a structure [137–141]. In Table 1 effects of *a/b* ratio and angle-ply of layers to maximize phase speed of nano-scaled plate are studied. As may be seen, the optimum amount of angle-ply in the laminated layers would be $\boldsymbol{\theta} = 37.5^{\circ}$. This would be due to the amount of phase speed in this angle-ply would be close to the highest amount of this factor in $\boldsymbol{\theta} = 45^{\circ}$. It should be note that, the optimization algorithm method can be a good tool for solving the complex structures and systems [142–146]. According to the mentioned table, it would be clear that by raising R_o/R_i ratio the optimum phase speed of the system would be declined.

4 Parametric results

In the presented section, a complete analysis has been conducted to illustrate the influences of different factors on the annular laminated micro-sized plate's frequency. The material characteristics of the laminated system have been illustrated in Table 2.

5 Validation study

The accuracy of the current results with the outcomes of published articles for different mode numbers, boundary conditions, and radius ratios are tabulated in Tables 3, 4, 5, and 6. As can be observed, the outputs of these tables show a good agreement between the outcomes of current research and Refs. [147–150] that the discrepancy is less than 2 percent. As well as the accuracy of the linear mode, for the correctness of the nonlinear frequency of the clamped annular plate made of isotropic material, Table 6 is presented. As can be seen, there is excellent accordance between the results of current research and mentioned References.

6 Results and discussion

The influences of elasticity modulus ratio (E_1/E_2) and material length scale factor (l/h) on the frequency of the laminated structure are reported in Fig. 5. According to Fig. 5 as the Young's modulus ratio increases the frequency of the current structure improves, exponentially and the mentioned impact is more considerable at the higher value of the material length scale parameter. In addition, it is true that the material length scale parameter has a positive impact on the dynamic responses of the structure but this impact is negligible when the Young's modulus ratio parameter is small. In addition, for a higher value of Young's modulus ratio the impact of material length scale parameter on the frequency of the current structure is much more remarkable than in the lower value of the E_1/E_2 parameter.

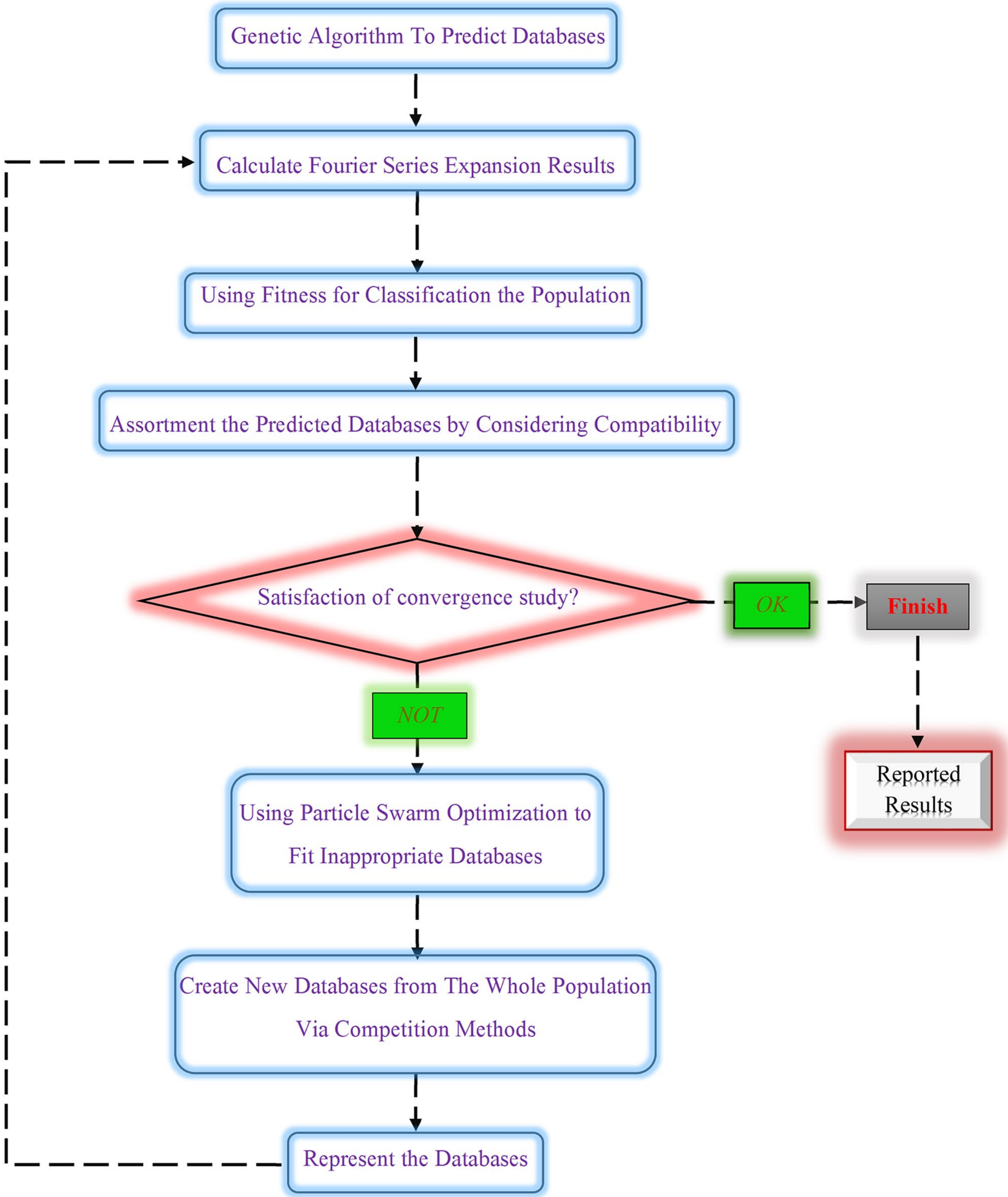

Fig. 4 The flowchart of optimization approach

Table 1 Optimum fibers orientations (Degree) and frequency (MHz) of annular microplate with different angle-ply of layers and R_o/R_i

R_o/R_i	θ=0°	θ=10°	θ=20°	θ=37.5°	θ=45°
2	1460	1471	1496	1599	1610
3	1359	1368	1379	1452	1460
4	1100	1120	1131	1231	1235
5	945	950	961	981	988

Frequency response of the current structure versus applied external load (F) is presented in Fig. 6 for various material length scale parameter. By having attention to Fig. 6 we can report that as the applied external load increases the frequency of the system decreases and the mentioned issue will continue till the buckling load appears. Also, increasing material length scale parameter is a reason for improving dynamic and static behavior or frequency and buckling load of the structure.

One of the aims of this study is displayed in Fig. 7 for investigation of the influences of radial mode number (n) on the frequency of the current structure. As Fig. 7 points out that it is true that increasing material length scale parameter has a positive impact on the dynamic information of the structure, but this impact can be bolded in the bigger radial mode numbers. Also, as the radial mode number increases, the frequency of the current structure improves.

The impacts of radius ratio (r_o/r_i) and material length scale parameters on the frequency of the current structure are reported in Fig. 8. According to Fig. 8 as the radius ratio increases, the frequency of the current structure decreases exponentially. In addition, in the lower value of the radius ratio, the material length scale parameter has a positive impact on the frequency of the structure, but in the higher value of the radius ratio, we can ignore the impact of l/h on the frequency of the current system.

In Fig. 9, influences of layers' angle-ply to maximize displacement of annular micro-scaled plates have been analyzed in detail. As it would be seen, the optimum amount of angle-ply in the laminated layers would be $\boldsymbol{\theta} = 37.5^{\circ}$. This would be due to the amount of displacement in this angle-ply would be close to minimizing the amount of this factor in $\boldsymbol{\theta} = 45^{\circ}$. According to the mentioned table, it would be clear that by raising the angle-ply, the structure's displacement would be smoother than less amount of it. Furthermore, as the mode number rises, the displacement field would be declined.

Table 3 Comparison of the first five dimensionless frequencies of an isotropic circular plate with clamped boundary condition and convergence and accuracy of DQ method is shown respect to the number of grid points. Dimensionless frequency $\omega^* = \omega r^2\sqrt{\rho h/D}$ where D is flexural rigidity $D = Eh^3/12(1-\nu^2)$

	ω_1^*	ω_2^*	ω_3^*	ω_4^*	ω_5^*
Ref. [147]	10.216	39.771	89.103	-	-
Ref. [148]	10.216	39.771	89.104	158.184	247.006
Ref [149]	10.2158	39.7711	89.1041	-	-
Current research (C.R)	10.1110	39.2749	89.6582	158.1109	246.9966

7 Conclusion

A general formulation was carried out to model linear vibrations of the laminated annular plate via higher order shear deformation theory in the current research. Also, characteristics of the frequency of an annular microplate made of laminated composite layers in the framework of MCST were investigated. The GDQE approach is employed to solve the governing equations of the micro-scaled structure through its boundary domains. For raising the performance of genetic algorithms to solve the problem, the particle swarm optimizer had been added as a GA's operator. The proposed mixed approach's convergency, accuracy, and applicability have been illustrated. Moreover, we demonstrate that for achieving the convergence outcome of the GA, PSO, and, we must assume higher than 23 iterations. Then, the most highlighted outcomes of this study would be as:

- for the higher value of elasticity modulus ratio, the impact of material length scale parameter on the frequency of the annular microplate is much more remarkable than in the less amount of the E_1/E_2 parameter
- as the radial mode number increases, the frequency of the current structure improves
- in the lower value of the radius ratio, the material length scale parameter has a positive impact on the frequency of the structure, but in the higher value of the radius ratio, we can ignore the impact of l/h on the frequency of the current system.
- the influence of the types of layering has to be assumed more than the influence of the number of layers on the annular laminate micro-scaled plate's amplitude

Table 2 Material properties of unidirectional glass fiber in a polyester resin matrix

Material properties	E_1	E_2	G_{12}	G_{13}	G_{23}	ρ_s	ν_s
Values	24.51GPa	7.77GPa	3.34 GPa	3.34 GPa	1.34 GPa	1800 kg/m^3	0.078

Table 4 Comparison of non-dimensional natural frequency of the annular plate for different axisymmetric vibration mode number, and inner radius to outer radius ratio for simply-simply boundary condition. ($h/R_i = 0.001$)

	R_i/R_o	Axisymmetric vibration mode number Simply-Simply				
		1	2	3	4	5
Ref. [150]	0.1	14.485	51.781	112.99	198.44	308.21
C.R	0.1	14.4257	50.9571	112.3096	197.6453	307.4021
Ref. [150]	0.2	16.780	63.370	140.60	248.62	387.44
C.R	0.2	16.0313	62.4648	139.6548	247.6486	386.4917
Ref. [150]	0.3	21.079	81.735	182.53	323.56	504.84
C.R	0.3	20.5176	81.1001	181.8785	322.9098	504.2238
Ref. [150]	0.4	28.122	110.56	247.69	439.61	686.32
C.R	0.4	27.6773	110.070	247.2045	439.1442	685.9137
Ref. [150]	0.5	40.043	158.64	356.06	632.39	987.60
C.R	0.5	39.6762	158.246	355.6866	632.0644	987.4015

Table 5 Comparison of non-dimensional natural frequency of the annular plate for different axisymmetric vibration mode number, and inner radius to outer radius ratio for clamped-simply boundary condition. ($h/Ri = 0.001$)

	R_i/R_o	Axisymmetric vibration mode number clamped-Simply				
		1	2	3	4	5
Ref. [150]	0.1	17.789	60.143	126.88	218.05	333.63
C.R	0.1	17.3622	59.4812	126.2196	217.3044	333.1126
Ref. [150]	0.2	22.714	76.542	161.22	276.78	423.20
C.R	0.2	22.4456	76.1638	160.9355	276.5130	423.2341
Ref. [150]	0.3	29.977	100.42	211.12	362.12	553.41
C.R	0.3	29.8039	100.1971	211.0576	362.1408	553.8186
Ref. [150]	0.4	41.193	137.15	287.88	493.44	753.80
C.R	0.4	41.0947	137.0520	288.0207	493.7325	754.6383
Ref. [150]	0.5	59.819	198.04	415.12	711.12	1086.0
C.R	0.5	59.7969	198.0706	415.5107	711.7848	1087.5

Table 6 Comparison of non-dimensional natural frequency of the annular plate for different axisymmetric vibration mode number, and inner radius to outer radius ratio for clamped–clamped boundary condition. ($h/Ri = 0.001$)

	R_i/R_o	Axisymmetric vibration mode number clamped–clamped				
		1	2	3	4	5
Ref. [150]	0.1	27.280	75.364	148.21	245.47	367.14
C.R	0.1	26.8273	74.8619	147.7355	245.3039	366.8225
Ref. [150]	0.2	34.609	95.738	188.14	311.40	465.53
C.R	0.2	34.3567	95.5770	188.1490	311.8589	466.0269
Ref. [150]	0.3	45.345	125.36	246.14	407.20	608.54
C.R	0.3	45.2147	125.4243	246.4927	408.1579	609.6949
Ref. [150]	0.4	61.871	170.89	335.34	554.59	828.64
C.R	0.4	61.8443	171.1903	336.0716	556.1585	830.5878
Ref. [150]	0.5	89.248	246.33	483.16	798.89	1193.5
C.R	0.5	89.3413	246.9347	484.4291	801.3773	1196.6

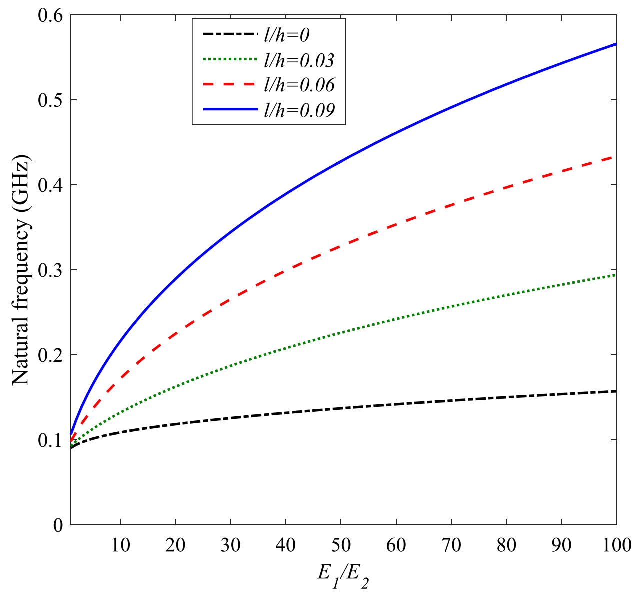

Fig. 5 Frequency of the current system versus E_1/E_2 value for various l/h parameter

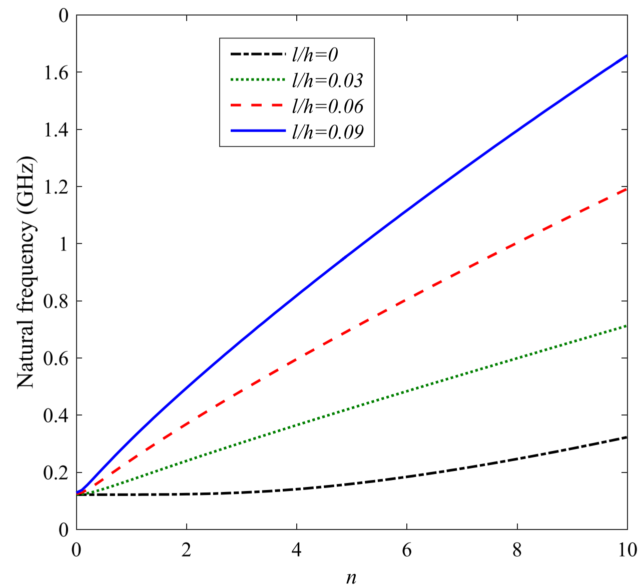

Fig. 7 Frequency of the current system versus radial mode number for various l/h

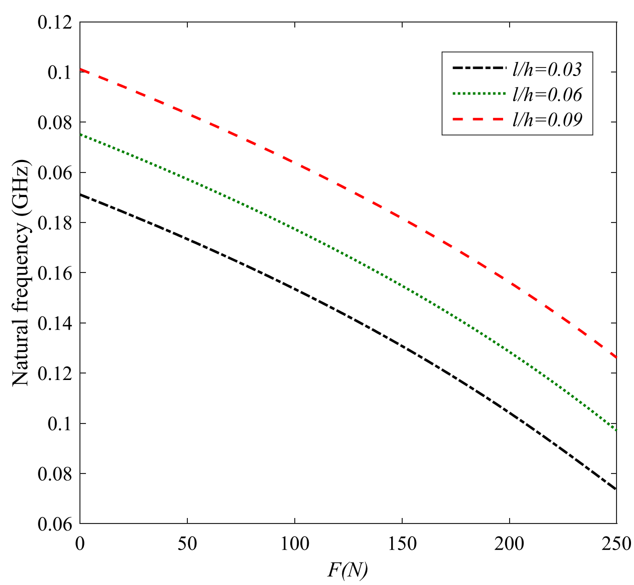

Fig. 6 Frequency of the current system versus F value for various l/h parameter

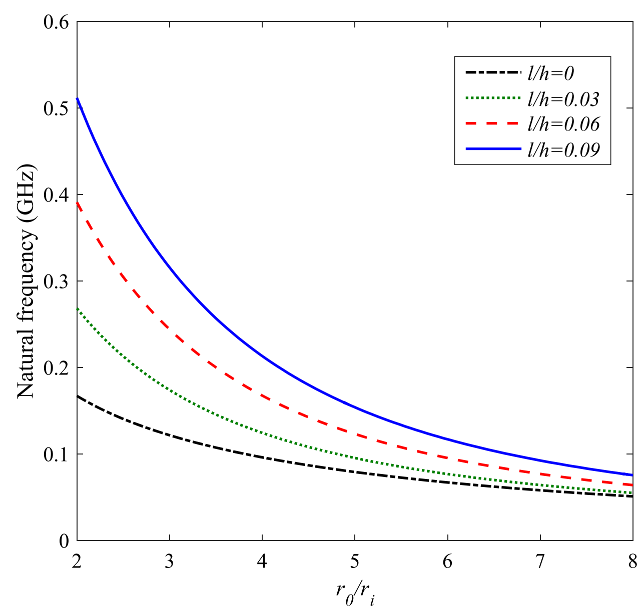

Fig. 8 The impacts of r_o/r_i and l/h parameters on the frequency of the current system

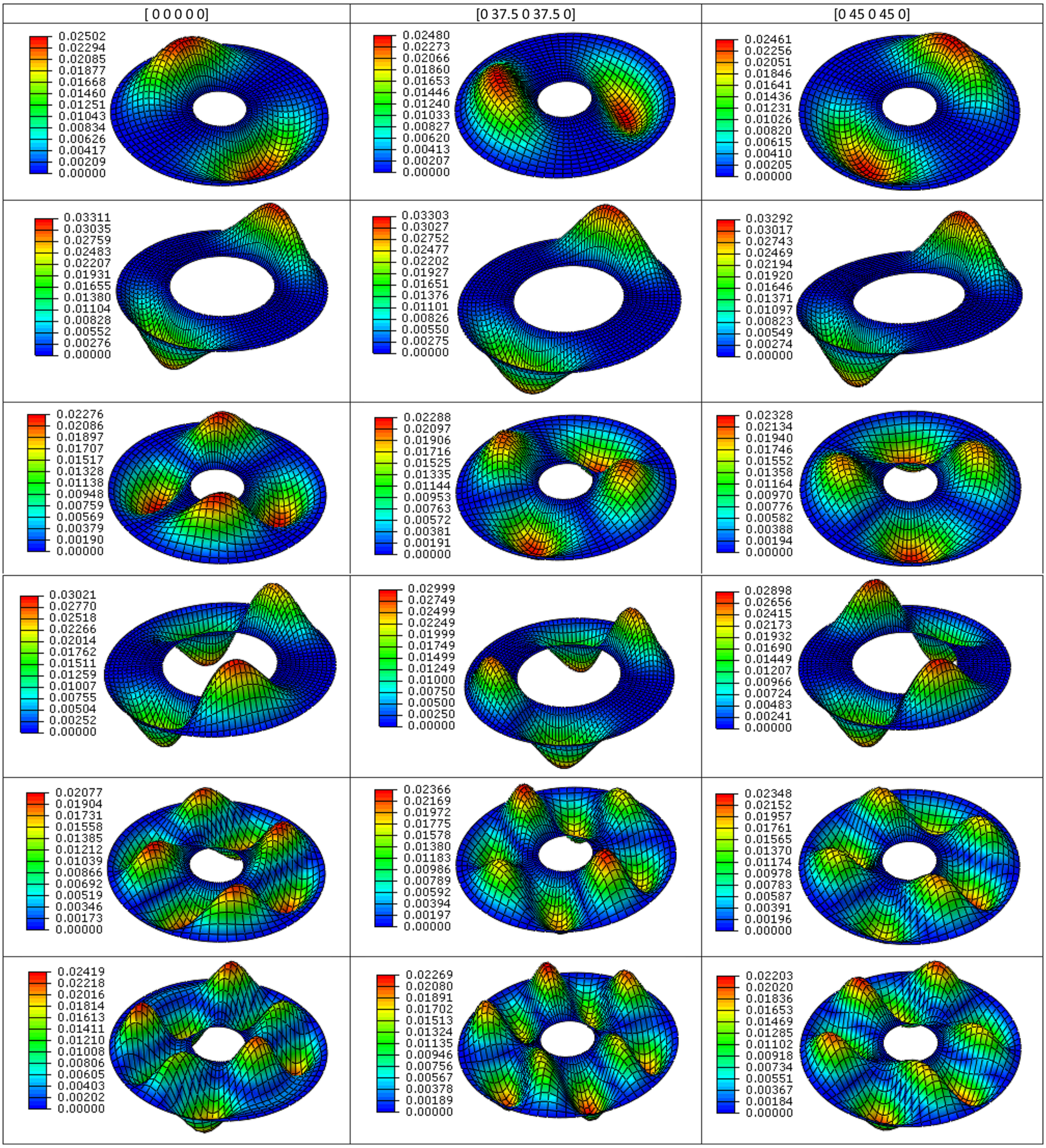

Fig. 9 Effects of different laminated patterns and angle ply on the deflection and deformation of the annular microplate

as the mode number raises, the displacement field would be declined

References:

1. Shen H, Zhang M, Wang H, Guo F, Susilo W (2021) A cloud-aided privacy-preserving multi-dimensional data comparison protocol. Inf Sci 545:739–752
2. Zenggang X, Zhiwen T, Xiaowen C, Xue-min Z, Kaibin Z, Conghuan Y (2019) Research on Image Retrieval Algorithm Based on Combination of Color and Shape Features. Journal of Signal Processing Systems:1–8
3. Mi C, Cao L, Zhang Z, Feng Y, Yao L, Wu Y (2020) A port container code recognition algorithm under natural conditions. Journal of Coastal Research 103 (SI):822–829
4. Zuo C, Chen Q, Tian L, Waller L, Asundi A (2015) Transport of intensity phase retrieval and computational imaging for partially coherent fields: The phase space perspective. Opt Lasers Eng 71:20–32
5. Mikhasev GI, Altenbach H (2019) Free Vibrations of Elastic Laminated Beams, Plates and Cylindrical Shells. In: Thin-walled Laminated Structures. Springer, pp 157–198. doi:https://doi.org/10.1007/978-3-030-12761-9_4
6. Karamanli A, Aydogdu M (2020) Free vibration and buckling analysis of laminated composites and sandwich microbeams using a transverse shear-normal deformable beam theory. Journal of Vibration and Control:1077546319878538
7. Zhao J, Liu J, Jiang J, Gao F (2020) Efficient deployment with geometric analysis for mmWave UAV communications. IEEE Wireless Commun Lett 9(7):1115–1119
8. Wang B, Cheng J (2018) Zhong S (2018) Bounded input bounded output stability for Lurie system with time-varying delay. Adv Difference Equ 1:1–13
9. Jiang Q, Shao F, Lin W, Gu K, Jiang G, Sun H (2017) Optimizing multistage discriminative dictionaries for blind image quality assessment. IEEE Trans Multimedia 20(8):2035–2048
10. Zhang L, Zheng H, Wan T, Shi D, Lyu L, Cai G (2021) An integrated control algorithm of power distribution for islanded microgrid based on improved virtual synchronous generator. IET Renewable Power Generation
11. Sinha L, Mishra S, Nayak A, Sahu S (2020) Free vibration characteristics of laminated composite stiffened plates: Experimental and numerical investigation. Composite Structures 233:111557
12. Xiang R, Pan Z-Z, Ouyang H, Zhang L-W (2020) A study of the vibration and lay-up optimization of rotating cross-ply laminated nanocomposite blades. Compos Struct 235:111775. https://doi.org/10.1016/j.compstruct.2019.111775
13. Moayedi H, Habibi M, Safarpour H, Safarpour M, Foong L (2020) Buckling and Frequency Responses of a Graphene Nanoplatelet Reinforced Composite Microdisk. International Journal of Applied Mechanics:1950102
14. Mou B, Bai Y, Patel V (2020) Post-local buckling failure of slender and over-design circular CFT columns with high-strength materials. Engineering Structures 210:110197
15. Metawa N, Elhoseny M, Hassan MK, Hassanien AE Loan portfolio optimization using genetic algorithm: a case of credit constraints. In: 2016 12th international computer engineering conference (ICENCO), 2016. IEEE, pp 59–64
16. Elhoseny M, Yuan X, El-Minir HK, Riad A Extending self-organizing network availability using genetic algorithm. In: Fifth international conference on computing, communications and networking technologies (ICCCNT), 2014. IEEE, pp 1–6
17. Tharwat A, Mahdi H, Elhoseny M, Hassanien AE (2018) Recognizing human activity in mobile crowdsensing environment using optimized k-NN algorithm. Expert Syst Appl 107:32–44
18. Abd El Aziz M, Hemdan AM, Ewees AA, Elhoseny M, Shehab A, Hassanien AE, Xiong S Prediction of biochar yield using adaptive neuro-fuzzy inference system with particle swarm optimization. In: 2017 IEEE PES PowerAfrica, 2017. IEEE, pp 115–120
19. Devaraj AFS, Elhoseny M, Dhanasekaran S, Lydia EL, Shankar K (2020) Hybridization of firefly and improved multi-objective particle swarm optimization algorithm for energy efficient load balancing in cloud computing environments. J Parallel Distrib Comput 142:36–45
20. Wang H, Zhang H, Dousti R, Safarpour H (2021) Dynamic simulation of moderately thick annular system coupled with shape memory alloy and multi-phase nanocomposite face sheets. Eng Comput. https://doi.org/10.1007/s00366-020-01246-x
21. Al-Furjan M, Bolandi SY, Habibi M, Ebrahimi F, Chen G, Safarpour H (2021) Enhancing vibration performance of a spinning smart nanocomposite reinforced microstructure conveying fluid flow. Engineering with Computers:1–16
22. Zare R, Najaafi N, Habibi M, Ebrahimi F, Safarpour H (2020) Influence of imperfection on the smart control frequency characteristics of a cylindrical sensor-actuator GPLRC cylindrical shell using a proportional-derivative smart controller. Smart Struct Syst 26(4):469–480
23. Liu H, Shen S, Oslub K, Habibi M, Safarpour H (2021) Amplitude motion and frequency simulation of a composite viscoelastic microsystem within modified couple stress elasticity. Engineering with Computers:1–15
24. Al-Furjan M, Dehini R, Paknahad M, Habibi M, Safarpour H (2021) On the nonlinear dynamics of the multi-scale hybrid nanocomposite-reinforced annular plate under hygro-thermal environment. Arch Civil Mech Eng 21(1):1–25. https://doi.org/10.1007/s43452-020-00151-w
25. Al-Furjan M, Habibi M, Ebrahimi F, Chen G, Safarpour M, Safarpour H (2020) A coupled thermomechanics approach for frequency information of electrically composite microshell using heat-transfer continuum problem. Eur Phys J Plus 135(10):1–45
26. Al-Furjan M, Habibi M, Ebrahimi F, Mohammadi K, Safarpour H (2020) Wave dispersion characteristics of high-speed-rotating laminated nanocomposite cylindrical shells based on four continuum mechanics theories. Waves in Random and Complex Media:1–27
27. Al-Furjan M, Habibi M, won Jung D, Safarpour H (2020) Vibrational characteristics of a higher-order laminated composite viscoelastic annular microplate via modified couple stress theory. Composite Structures:113152
28. Al-Furjan M, Oyarhossein MA, Habibi M, Safarpour H, Jung DW (2020) Wave propagation simulation in an electrically open shell reinforced with multi-phase nanocomposites. Engineering with Computers:1–17. doi:https://doi.org/10.1007/s00366-020-01167-9
29. Civalek Ö, Baltacıoglu AK (2019) Free vibration analysis of laminated and FGM composite annular sector plates. Compos B Eng 157:182–194. https://doi.org/10.1016/j.compositesb.2018.08.101
30. Sheng H, Wang S, Zhang Y, Yu D, Cheng X, Lyu W, Xiong Z (2020) Near-online Tracking with Co-occurrence Constraints in Blockchain-based Edge Computing. IEEE Internet of Things Journal
31. Lv Z, Qiao L, Hossain MS, Choi BJ (2021) Analysis of using blockchain to protect the privacy of drone big data. IEEE Network 35(1):44–49
32. Lv Z, Singh AK, Li J (2021) Deep learning for security problems in 5G heterogeneous networks. IEEE Network 35(2):67–73

33. Lv Z, Qiao L, Song H (2020) Analysis of the security of Internet of multimedia things. ACM Trans Multimed Comput Commun Appl (TOMM) 16(3s):1–16
34. Mohammadimehr M, Afshari H, Salemi M, Torabi K, Mehrabi M (2019) Free vibration and buckling analyses of functionally graded annular thin sector plate in-plane loads using GDQM. Struct Eng Mech 71(5):525–544. https://doi.org/10.12989/sem.2019.71.5.525
35. Arshid E, Kiani A, Amir S (2019) Magneto-electro-elastic vibration of moderately thick FG annular plates subjected to multi-physical loads in thermal environment using GDQ method by considering neutral surface. Proc Inst Mech Eng Part L 233(10):2140–2159. https://doi.org/10.1177/1464420719832626
36. Lv Z, Qiao L, Singh AK, Wang Q (2021) Fine-grained visual computing based on deep learning. ACM Trans Multim Comput Commun Appl 17(1s):1–19
37. Medvedeva MA, Simos T, Tsitouras C (2021) Exponential integrators for linear inhomogeneous problems. Math Methods Appl Sci 44(1):937–944
38. Medvedeva MA, Simos T, Tsitouras C (2021) Sixth-order, P-stable, Numerov-type methods for use at moderate accuracies. Math Methods Appl Sci 44(8):6923–6930
39. Medvedev MA, Simos T, Tsitouras C (2020) Explicit, eighth-order, four-step methods for solving $$ y^{\prime\prime}= f (x, y) $$ y ″= f (x, y). Bull Malays Math Sci Soc 43(5):3791–3807
40. Vinyas M (2020) On frequency response of porous functionally graded magneto-electro-elastic circular and annular plates with different electro-magnetic conditions using HSDT. Compos Struct 240:112044
41. Simos T, Tsitouras C (2020) Explicit, ninth order, two-step methods for solving inhomogeneous linear problems x ″(t)= Λx (t)+ f (t). Appl Numer Math 153:344–351
42. Kovalnogov VN, Simos TE, Tsitouras C (2020) Ninth-order, explicit, two-step methods for second-order inhomogeneous linear IVPs. Math Methods Appl Sci 43(7):4918–4926
43. Hou CC, Simos TE, Famelis IT (2020) Neural network solution of pantograph type differential equations. Math Methods Appl Sci 43(6):3369–3374
44. Safarpour M, Rahimi A, Alibeigloo A (2019) Static and free vibration analysis of graphene platelets reinforced composite truncated conical shell, cylindrical shell, and annular plate using theory of elasticity and DQM. Mechanics Based Design of Structures and Machines:1–29. doi:https://doi.org/10.1080/15397734.2019.1646137
45. Lv Z, Lou R, Li J, Singh AK, Song H (2021) Big data analytics for 6G-enabled massive internet of things. IEEE Internet Things J 8(7):5350–5359
46. Lou R, Lv Z, Dang S, Su T, Li X (2021) Application of machine learning in ocean data. Multimedia Systems:1–10
47. Lv Z, Chen D, Li J (2021) Novel system design and implementation for the smart city vertical market. IEEE Commun Mag 59(4):126–131
48. Lv Z, Chen D, Lou R, Alazab A (2021) Artificial intelligence for securing industrial-based cyber–physical systems. Futur Gener Comput Syst 117:291–298
49. Dai T, Yang Y, Dai H-L, Tang H, Lin Z-Y (2019) Hygrothermal mechanical behaviors of a porous FG-CRC annular plate with variable thickness considering aggregation of CNTs. Compos Struct 215:198–213. https://doi.org/10.1016/j.compstruct.2019.02.061
50. Elhoseny M, Shankar K, Uthayakumar J (2019) Intelligent diagnostic prediction and classification system for chronic kidney disease. Sci Rep 9(1):1–14
51. Abdel-Basset M, Mohamed M, Elhoseny M, Chiclana F, Zaied AE-NH (2019) Cosine similarity measures of bipolar neutrosophic set for diagnosis of bipolar disorder diseases. Artif Intell Med 101:101735
52. Zaher M, Shehab A, Elhoseny M, Farahat FF (2020) Unsupervised model for detecting plagiarism in internet-based handwritten Arabic documents. Journal of Organizational and End User Computing (JOEUC) 32(2):42–66
53. Lakshmanaprabu S, Elhoseny M, Shankar K (2019) Optimal tuning of decentralized fractional order PID controllers for TITO process using equivalent transfer function. Cogn Syst Res 58:292–303
54. Krishnaraj N, Elhoseny M, Thenmozhi M, Selim MM, Shankar K (2020) Deep learning model for real-time image compression in Internet of Underwater Things (IoUT). J Real-Time Image Proc 17(6):2097–2111
55. Eshraghi I, Dag S (2020) Forced vibrations of functionally graded annular and circular plates by domain-boundary element method. J Appl Math Mech (Zeitschrift für Angewandte Mathematik und Mechanik. https://doi.org/10.1002/zamm.201900048
56. Bemani Khouzestani L, Khorshidvand AR (2019) Axisymmetric free vibration and stress analyses of saturated porous annular plates using generalized differential quadrature method. J Vib Control 25(21–22):2799–2818. https://doi.org/10.1177/1077546319871132
57. Javani M, Kiani Y, Eslami M (2020) Thermal buckling of FG graphene platelet reinforced composite annular sector plates. Thin-Walled Struct 148:106589. https://doi.org/10.1016/j.tws.2019.106589
58. Heshmati M, Jalali S (2019) Effect of radially graded porosity on the free vibration behavior of circular and annular sandwich plates. Eur J Mech A 74:417–430
59. Al-Furjan MSH, Moghadam SA, Dehini R, Shan L, Habibi M, Safarpour H (2020) Vibration control of a smart shell reinforced by graphene nanoplatelets under external load: Semi-numerical and finite element modeling. Thin-Walled Structures. https://doi.org/10.1016/j.tws.2020.107242
60. Al-Furjan M, Habibi M, won Jung D, Safarpour H, Safarpour M (2020) On the buckling of the polymer-CNT-fiber nanocomposite annular system under thermo-mechanical loads. Mech Based Des Struct Machines 1–21
61. Al-Furjan M, Habibi M, won Jung D, Chen G, Safarpour M, Safarpour H, (2020) Chaotic responses and nonlinear dynamics of the graphene nanoplatelets reinforced doubly-curved panel. Eur J Mech A 85:104091
62. Al-Furjan M, Oyarhossein MA, Habibi M, Safarpour H, Jung DW (2020) Frequency and critical angular velocity characteristics of rotary laminated cantilever microdisk via two-dimensional analysis. Thin-Walled Struct 157:107111
63. Al-Furjan M, Mohammadgholiha M, Alarifi IM, Habibi M, Safarpour H (2020) On the phase velocity simulation of the multi curved viscoelastic system via an exact solution framework. Eng Comput. https://doi.org/10.1007/s00366-020-01152-2
64. Lori ES, Ebrahimi F, Supeni EEB, Habibi M, Safarpour H (2020) The critical voltage of a GPL-reinforced composite microdisk covered with piezoelectric layer. Engineering with Computers:1–20
65. Al-Furjan M, Habibi M, Safarpour H (2020) Vibration control of a smart shell reinforced by graphene nanoplatelets. Int J Appl Mech. https://doi.org/10.1142/S1758825120500660
66. Moayedi H, Aliakbarlou H, Jebeli M, Noormohammadiarani O, Habibi M, Safarpour H, Foong L (2020) Thermal buckling responses of a graphene reinforced composite micropanel structure. Int J Appl Mech 12(01):2050010
67. Oyarhossein MA, Aa A, Habibi M, Makkiabadi M, Daman M, Safarpour H, Jung DW (2020) Dynamic response of the nonlocal strain-stress gradient in laminated polymer composites microtubes. Sci Rep 10(1):1–19

68. Habibi M, Safarpour M, Safarpour H (2020) Vibrational characteristics of a FG-GPLRC viscoelastic thick annular plate using fourth-order Runge-Kutta and GDQ methods. Mech Based Des Struct Mach. 1–22
69. Ebrahimi F, Supeni EEB, Habibi M, Safarpour H (2020) Frequency characteristics of a GPL-reinforced composite microdisk coupled with a piezoelectric layer. Eur Phys J Plus 135(2):144
70. Mohammad-Rezaei Bidgoli E, Arefi M (2019) Free vibration analysis of micro plate reinforced with functionally graded graphene nanoplatelets based on modified strain-gradient formulation. J Sandwich Struct Mater. https://doi.org/10.1177/1099636219839302
71. Sheng D, Zhang S, Yu Z, Zhang J (2013) Assessing frost susceptibility of soils using PCHeave. Cold Reg Sci Technol 95:27–38
72. Zhou M, Li Y, Tahir MJ, Geng X, Wang Y, He W (2021) Integrated Statistical Test of Signal Distributions and Access Point Contributions for Wi-Fi Indoor Localization. IEEE Transactions on Vehicular Technology
73. Zhou M, Wang Y, Liu Y, Tian Z (2019) An information-theoretic view of WLAN localization error bound in GPS-denied environment. IEEE Trans Veh Technol 68(4):4089–4093
74. Zhou M, Li X, Wang Y, Li S, Ding Y, Nie W (2020) 6G Multisource Information Fusion Based Indoor Positioning via Gaussian Kernel Density Estimation. IEEE Internet of Things Journal
75. Mahinzare M, Alipour MJ, Sadatsakkak SA, Ghadiri M (2019) A nonlocal strain gradient theory for dynamic modeling of a rotary thermo piezo electrically actuated nano FG circular plate. Mech Syst Signal Process 115:323–337. https://doi.org/10.1016/j.ymssp.2018.05.043
76. Tang Y, Elhoseny M (2019) Computer network security evaluation simulation model based on neural network. J Intell Fuzzy Syst 37(3):3197–3204
77. Puri V, Jha S, Kumar R, Priyadarshini I, Abdel-Basset M, Elhoseny M, Long HV (2019) A hybrid artificial intelligence and internet of things model for generation of renewable resource of energy. IEEE Access 7:111181–111191
78. Libo Z, Tian H, Chunyun G, Elhoseny M (2019) Real-time detection of cole diseases and insect pests in wireless sensor networks. J Intell Fuzzy Syst 37(3):3513–3524
79. Cao B, Zhao J, Yang P, Yang P, Liu X, Qi J, Simpson A, Elhoseny M, Mehmood I, Muhammad K (2019) Multiobjective feature selection for microarray data via distributed parallel algorithms. Futur Gener Comput Syst 100:952–981
80. Dorri A, Kanhere SS, Jurdak R (2019) MOF-BC: a memory optimized and flexible blockchain for large scale networks. Futur Gener Comput Syst 92:357–373
81. Arshid E, Amir S, Loghman A (2020) Static and dynamic analyses of FG-GNPs reinforced porous nanocomposite annular micro-plates based on MSGT. Int J Mech Sci. https://doi.org/10.1016/j.ijmecsci.2020.105656
82. Pal S, Das D (2020) Free vibration behavior of rotating bidirectional functionally-graded micro-disk for flexural and torsional modes in thermal environment. Int J Mech Sci. https://doi.org/10.1016/j.ijmecsci.2020.105635
83. Qi L, Huang S, Fu G, Li A, Zhou S, Jiang X (2019) Modeling of the flexoelectric annular microplate based on strain gradient elasticity theory. Mech Adv Mater Struct 26(23):1958–1968
84. Alinaghizadeh F, Shariati M (2020) Nonlinear analysis of size-dependent annular sector and rectangular microplates under transverse loading and resting on foundations based on the modified couple stress theory. Thin-Walled Structures 149:106583
85. Thakur S, Singh AK, Ghrera SP, Elhoseny M (2019) Multi-layer security of medical data through watermarking and chaotic encryption for tele-health applications. Multimed Tools Appl 78(3):3457–3470
86. Abdel-Basset M, El-Hoseny M, Gamal A, Smarandache F (2019) A novel model for evaluation Hospital medical care systems based on plithogenic sets. Artif Intell Med 100:101710
87. Dutta AK, Elhoseny M, Dahiya V, Shankar K (2020) An efficient hierarchical clustering protocol for multihop Internet of vehicles communication. Transact Emerg Telecommun Technol 31(5):e3690
88. Shankar K, Elhoseny M (2019) Trust based cluster head election of secure message transmission in MANET using multi secure protocol with TDES. J UCS 25(10):1221–1239
89. Elhoseny M, Bian G-B, Lakshmanaprabu S, Shankar K, Singh AK, Wu W (2019) Effective features to classify ovarian cancer data in internet of medical things. Comput Netw 159:147–156
90. Elhoseny M, Shankar K (2019) Optimal bilateral filter and convolutional neural network based denoising method of medical image measurements. Measurement 143:125–135
91. Mohammadimehr M, Emdadi M, Rousta Navi B (2020) Dynamic stability analysis of microcomposite annular sandwich plate with carbon nanotube reinforced composite facesheets based on modified strain gradient theory. J Sandwich Struct Mater 22(4):1199–1234
92. Alipour M, Shariyat M (2019) Nonlocal zigzag analytical solution for Laplacian hygrothermal stress analysis of annular sandwich macro/nanoplates with poor adhesions and 2D-FGM porous cores. Arch Civil Mech Eng 19(4):1211–1234. https://doi.org/10.1016/j.acme.2019.06.008
93. Bagheri E, Jahangiri M, Asghari M (2020) Effects of couple stresses on the in-plane vibration of micro-rotating disks. Journal of Vibration and Control:1077546319892426
94. Yuan X, Li D, Mohapatra D, Elhoseny M (2018) Automatic removal of complex shadows from indoor videos using transfer learning and dynamic thresholding. Comput Electr Eng 70:813–825
95. Gaber T, Abdelwahab S, Elhoseny M, Hassanien AE (2018) Trust-based secure clustering in WSN-based intelligent transportation systems. Comput Netw 146:151–158
96. Mehrabi P, Shariati M, Kabirifar K, Jarrah M, Rasekh H, Trung NT, Shariati A, Jahandari S (2021) Effect of pumice powder and nano-clay on the strength and permeability of fiber-reinforced pervious concrete incorporating recycled concrete aggregate. Construct Build Mater 287:122652
97. Shariati M, Armaghani DJ, Khandelwal M, Zhou J, Eyvaziyan A, Khorami M (2021) Assessment of longstanding effects of fly ash and silica fume on the compressive strength of concrete using extreme learning machine and artificial neural network. J Adv Eng Comput 5(1):50–75
98. Nouri K, Sulong NR, Ibrahim Z, Shariati M (2021) Behaviour of novel stiffened angle shear connectors at ambient and elevated temperatures. Adv Steel Construct 17(1):28–38
99. Rajaei S, Shoaei P, Shariati M, Ameri F, Musaeei HR, Behforouz B, de Brito J (2021) Rubberized alkali-activated slag mortar reinforced with polypropylene fibres for application in lightweight thermal insulating materials. Construction and Building Materials 270:121430
100. Yazdani M, Kabirifar K, Frimpong BE, Shariati M, Mirmozaffari M, Boskabadi A (2021) Improving construction and demolition waste collection service in an urban area using a simheuristic approach: A case study in Sydney. Australia. J Clean Product 280:124138
101. Afshar A, Jahandari S, Rasekh H, Shariati M, Afshar A, Shokrgozar A (2020) Corrosion resistance evaluation of rebars with various primers and coatings in concrete modified with different additives. Construct Build Mater 262:120034
102. Toghroli A, Mehrabi P, Shariati M, Trung NT, Jahandari S, Rasekh H (2020) Evaluating the use of recycled concrete aggregate and pozzolanic additives in fiber-reinforced pervious

concrete with industrial and recycled fibers. Construct Build Mater 252:118997
103. Safa M, Sari PA, Shariati M, Suhatril M, Trung NT, Wakil K, Khorami M (2020) Development of neuro-fuzzy and neuro-bee predictive models for prediction of the safety factor of eco-protection slopes. Phys A 550:124046
104. Reddy JN (2003) Mechanics of laminated composite plates and shells: theory and analysis. CRC Press
105. Shariati A, Ghabussi A, Habibi M, Safarpour H, Safarpour M, Tounsi A, Safa M (2020) Extremely large oscillation and nonlinear frequency of a multi-scale hybrid disk resting on nonlinear elastic foundation. Thin-Walled Structures 154:106840. https://doi.org/10.1016/j.tws.2020.106840
106. Chen H, Song H, Li Y, Safarpour M (2020) Hygro-thermal buckling analysis of polymer–CNT–fiber-laminated nanocomposite disk under uniform lateral pressure with the aid of GDQM. Engineering with Computers:1–25
107. Moradi Z, Davoudi M, Ebrahimi F, Ehyaei AF (2021) Intelligent wave dispersion control of an inhomogeneous micro-shell using a proportional-derivative smart controller. Waves in Random and Complex Media:1–24
108. Huang X, Zhang Y, Moradi Z, Shafiei N (2021) Computer simulation via a couple of homotopy perturbation methods and the generalized differential quadrature method for nonlinear vibration of functionally graded non-uniform micro-tube. Eng Comput 1–18
109. Zhao Y, Moradi Z, Davoudi M, Zhuang J Bending and stress responses of the hybrid axisymmetric system via state-space method and 3D-elasticity theory. Engineering with Computers:1–23
110. Ma L, Liu X, Moradi Z On the chaotic behavior of graphene-reinforced annular systems under harmonic excitation. Engineering with Computers:1–25
111. Huang X, Zhu Y, Vafaei P, Moradi Z, Davoudi M (2021) An iterative simulation algorithm for large oscillation of the applicable 2D-electrical system on a complex nonlinear substrate. Engineering with Computers:1–13
112. Jiao J, Ghoreishi S-m, Moradi Z, Oslub K (2021) Coupled particle swarm optimization method with genetic algorithm for the static–dynamic performance of the magneto-electro-elastic nanosystem. Engineering with Computers:1–15
113. Barooti MM, Safarpour H, Ghadiri M (2017) Critical speed and free vibration analysis of spinning 3D single-walled carbon nanotubes resting on elastic foundations. Eur Phys J Plus 132(1):6. https://doi.org/10.1140/epjp/i2017-11275-5
114. Jiang D, Wang F, Lv Z, Mumtaz S, Al-Rubaye S, Tsourdos A, Dobre O (2021) QoE-Aware Efficient Content Distribution Scheme for Satellite-Terrestrial Networks. IEEE Transactions on Mobile Computing
115. Lou R, Wang W, Li X, Zheng Y, Lv Z (2021) Prediction of Ocean Wave Height Suitable for Ship Autopilot. IEEE Transactions on Intelligent Transportation Systems
116. Li Y, Qiao L, Lv Z (2021) An Optimized Byzantine Fault Tolerance Algorithm for Consortium Blockchain. Peer-to-Peer Networking and Applications:1–14
117. Yu Z, Amin SU, Alhussein M, Lv Z (2021) Research on disease prediction based on improved DeepFM and IoMT. IEEE Access 9:39043–39054
118. Shu C (2012) Differential quadrature and its application in engineering. Springer Science & Business Media,
119. Tornabene F, Fantuzzi N, Ubertini F, Viola E (2015) Strong formulation finite element method based on differential quadrature: a survey. Applied Mechanics Reviews 67 (2). doi:https://doi.org/10.1115/1.4028859
120. Jiao J, Ghoreishi S-m, Moradi Z, Oslub K (2021) Coupled particle swarm optimization method with genetic algorithm for the static–dynamic performance of the magneto-electro-elastic nanosystem. Engineering with Computers. https://doi.org/10.1007/s00366-021-01391-x
121. Kennedy J, Eberhart R (1995) Particle swarms optimization In IEEE International Conference on Neural Networks, vol. 4.
122. Elhoseny M, Shehab A, Yuan X (2017) Optimizing robot path in dynamic environments using genetic algorithm and bezier curve. Journal of Intelligent & Fuzzy Systems 33(4):2305–2316
123. Hosseinabadi AAR, Vahidi J, Saemi B, Sangaiah AK, Elhoseny M (2019) Extended genetic algorithm for solving open-shop scheduling problem. Soft Comput 23(13):5099–5116
124. Elsayed W, Elhoseny M, Sabbeh S, Riad A (2018) Self-maintenance model for wireless sensor networks. Comput Electr Eng 70:799–812
125. Rizk-Allah RM, Hassanien AE, Elhoseny M (2018) A multi-objective transportation model under neutrosophic environment. Comput Electr Eng 69:705–719
126. Krishnaraj N, Elhoseny M, Lydia EL, Shankar K, ALDabbas O (2021) An efficient radix trie-based semantic visual indexing model for large-scale image retrieval in cloud environment. Software: Practice and Experience 51 (3):489–502
127. Mohanty SN, Lydia EL, Elhoseny M, Al Otaibi MMG, Shankar K (2020) Deep learning with LSTM based distributed data mining model for energy efficient wireless sensor networks. Physical Communication 40:101097
128. Elhoseny H, Elhoseny M, Riad AM, Hassanien AEA (2018) framework for big data analysis in smart cities. International conference on advanced machine learning technologies and applications. Springer, pp 405–414
129. Shankar K, Elhoseny M, Lakshmanaprabu S, Ilayaraja M, Vidhyavathi R, Elsoud MA, Alkhambashi M (2020) Optimal feature level fusion based ANFIS classifier for brain MRI image classification. CONCURRENCY AND COMPUTATION-PRACTICE & EXPERIENCE 32 (1)
130. Ewees AA, Abd El Aziz M, Elhoseny M Social-spider optimization algorithm for improving ANFIS to predict biochar yield. In: 2017 8th international conference on computing, communication and networking technologies (ICCCNT), 2017. IEEE, pp 1–6
131. Xu X, Cao D, Zhou Y, Gao J (2020) Application of neural network algorithm in fault diagnosis of mechanical intelligence. Mechanical Systems and Signal Processing 141:106625
132. Abdel-Basset M, Mohamed R, Elhoseny M, Chakrabortty RK, Ryan M (2020) A hybrid COVID-19 detection model using an improved marine predators algorithm and a ranking-based diversity reduction strategy. IEEE Access 8:79521–79540
133. Saračević M, Adamović S, Maček N, Elhoseny M, Sarhan S (2020) Cryptographic keys exchange model for smart city applications. IET Intel Transport Syst 14(11):1456–1464
134. Uthayakumar J, Elhoseny M, Shankar K (2020) Highly reliable and low-complexity image compression scheme using neighborhood correlation sequence algorithm in WSN. IEEE Trans Reliab 69(4):1398–1423
135. El-Hasnony IM, Barakat SI, Elhoseny M, Mostafa RR (2020) Improved feature selection model for big data analytics. IEEE Access 8:66989–67004
136. Ali M, Jung LT, Abdel-Aty A-H, Abubakar MY, Elhoseny M, Ali I (2020) Semantic-k-NN algorithm: An enhanced version of traditional k-NN algorithm. Expert Systems with Applications 151:113374
137. Elhoseny M (2020) Intelligent firefly-based algorithm with Levy distribution (FF-L) for multicast routing in vehicular communications. Expert Systems with Applications 140:112889
138. Elhoseny M (2020) Multi-object detection and tracking (MODT) machine learning model for real-time video surveillance systems. Circuits Systems Signal Process 39(2):611–630

139. Geetha K, Anitha V, Elhoseny M, Kathiresan S, Shamsolmoali P, Selim MM (2021) An evolutionary lion optimization algorithm-based image compression technique for biomedical applications. Expert Systems 38 (1):e12508
140. Lydia EL, Raj JS, Pandi Selvam R, Elhoseny M, Shankar K (2021) Application of discrete transforms with selective coefficients for blind image watermarking. Transactions on Emerging Telecommunications Technologies 32 (2):e3771
141. Elhoseny M, Shankar K (2019) Reliable data transmission model for mobile ad hoc network using signcryption technique. IEEE Trans Reliab 69(3):1077–1086
142. Valayapalayam Kittusamy SR, Elhoseny M, Kathiresan S (2019) An enhanced whale optimization algorithm for vehicular communication networks. International Journal of Communication Systems:e3953
143. Muhammad K, Khan S, Elhoseny M, Ahmed SH, Baik SW (2019) Efficient fire detection for uncertain surveillance environment. IEEE Trans Industr Inf 15(5):3113–3122
144. Eassa AM, Elhoseny M, El-Bakry HM, Salama AS (2018) NoSQL injection attack detection in web applications using RESTful service. Program Comput Softw 44(6):435–444
145. Murugan B, Elhoseny M, Shankar K, Uthayakumar J (2019) Region-based scalable smart system for anomaly detection in pedestrian walkways. Comput Electr Eng 75:146–160
146. Hurrah NN, Parah SA, Loan NA, Sheikh JA, Elhoseny M, Muhammad K (2019) Dual watermarking framework for privacy protection and content authentication of multimedia. Futur Gener Comput Syst 94:654–673
147. Azimi S (1988) Free vibration of circular plates with elastic edge supports using the receptance method. J Sound Vib 120(1):19–35. https://doi.org/10.1016/0022-460X(88)90332-X
148. Wu T, Wang Y, Liu G (2002) Free vibration analysis of circular plates using generalized differential quadrature rule. Comput Methods Appl Mech Eng 191(46):5365–5380. https://doi.org/10.1016/S0045-7825(02)00463-2
149. Lal R, Ahlawat N (2015) Axisymmetric vibrations and buckling analysis of functionally graded circular plates via differential transform method. European Journal of Mechanics-A/Solids 52:85–94
150. Han J-B, Liew K (1999) Axisymmetric free vibration of thick annular plates. Int J Mech Sci 41(9):1089–1109. https://doi.org/10.1016/S0020-7403(98)00057-5